Chromophore Orientation Dynamics, Phase Stability, and Photorefractive Effects in Branched Azobenzene Chromophores

Victoria E. Campbell,[†] Insik In,[†] David J. McGee,[‡] Nathaniel Woodward,[‡] Anthony Caruso,[‡] and Padma Gopalan*,[†]

Materials Science and Engineering, University of Wisconsin−Madison, Wisconsin 53706, and Department of Physics, Drew University, Madison, New Jersey 07940

Received August 10, 2005; Revised Manuscript Received November 13, 2005

ABSTRACT: The increased solubility and uniform dispersal of branched azobenzene chromophores over their monomeric analogues have been shown to improve the electrooptic performance of high glass transition temperature (T_g) blended polymers. We report here the application of these branched chromophores as guest nonlinear optical molecules in the plasticized low-T_g photoconducting host polymer poly(vinylcarbazole) and demonstrate the presence of orientationally enhanced photorefractive index gratings. When compared with their monomeric analogues, branched chromophores were compatible over a broader range of concentrations and resulted in higher quality optical films; these films have retained their optical clarity for 1 year. A new branched electrooptic chromophore with r_{33} of 14 pm/V at 1550 nm was synthesized and exhibited photorefractive two-beam coupling over a range of applied fields, including a net two-beam coupling amplification coefficient of 6.4 cm^{-1} at 780 nm.

Introduction

Electro-optic polymers can alter the speed of light via an electrically controlled refractive index and are the subject of intense research for use in photonic applications such as optical modulation. A particularly successful design paradigm involves blending nonlinear optical chromophores with an appropriate polymer host and employing electric field poling to induce orientational ordering of the dipolar chromophores. To achieve macroscopic electrooptic activity sufficient for applications, careful control of chromophore shape is necessary to minimize the inter-chromophore interactions that lead to antiparallel aggregation. For example, dendritic stilbene chromophores have been blended with amorphous polycarbonate to produce macroscopic electrooptic coefficients exceeding 100 pm/V.[1] The three-dimensional architecture of such chromophores provides effective site isolation, inhibiting antiparallel aggregation.[2] We have recently synthesized branched azobenzene chromophores that offer the site isolation of synthetically more complex dendritic structures while providing some measure of photostability common to azo dyes. These chromophores were soluble in an amorphous polycarbonate host and exhibited electro-optic coefficients from 9 to 27 pm/V at 1550 nm. Synthesis was carried out in six or seven steps with an overall yield of around 80%. Studies on these chromophores revealed a strong dependence of the electrooptic coefficient on the host matrix.[3]

Characteristics such as spherical morphology, increased solubility, and effective site isolation of functional units attributed to dendritic[4] and to some extent branched chromophores make them useful for applications in permanently poled electro-optic polymers. Likewise, these same characteristics also make them useful in low glass transition temperature (T_g) systems that exhibit light-induced refractive index variations via the photorefractive effect. Photorefractive polymers consist of a photoconducting polymer host blended with an electrooptic chromophore. Illumination with an optical intensity grating causes a charge redistribution and subsequent space-charge electric field over the region of illumination. The space-charge field alters the refractive index via the electro-optic effect. Additionally, in low-T_g photorefractive polymers the chromophore is orientationally mobile and will be periodically reoriented by the spatially varying local electric field. This gives rise to a spatially modulated birefringence which can provide a significant contribution to the overall refractive index modulation.[5]

Our previous studies have indicated that branched chromophores were compatible only with selective hosts such as amorphous polycarbonate. This suggests that a polar branched chromophore with aromatic core would likely be compatible with a polar aromatic polymer host commonly used in photorefractive polymer systems such as poly(vinylcarbazole) (PVK). On the basis of these observations, we report here a study of branched azobenzene chromophore/PVK blends and provide experimental evidence that photorefractive index gratings can be induced in these blends with laser light in the 676−780 nm range. We also report the synthesis of a new branched chromophore with a modified acceptor group designed to increase electro-optic activity and discuss its utility as a photorefractive chromophore. We discuss the phase stability of the blends, chromophore orientational dynamics, and the photorefractive index dynamics. When compared with their monomeric analogues, branched chromophores offer improvements in film quality, blend stability, and overall photorefractive performance as measured by diffraction efficiency and two-beam coupling experiments.

Experimental Section

Materials. All the chemicals were purchased from Aldrich and were used without further purification, with the exception of ethylcarbazole, which was purified via recrystallization.

General Methods of Material Characterization. ^{1}H NMR was taken on a Bruker 360 MHz with tetramethylsilane as internal standard. UV−vis spectra were obtained from the HP 8453 UV−vis system. Elemental analysis was performed by Robertson Microlit

* To whom correspondence should be addressed. E-mail: pgopalan@wisc.edu.
[†] University of Wisconsin−Madison.
[‡] Drew University.

10.1021/ma051772o CCC: $33.50
Published on Web 01/04/2006

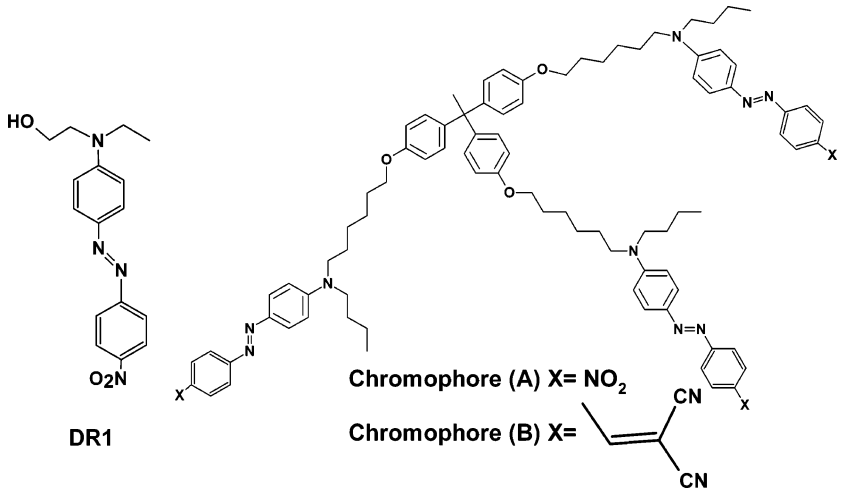

Figure 1. Structure of the three azobenzene chromophores studied.

Scheme 1. Synthetic Scheme for Chromophore B

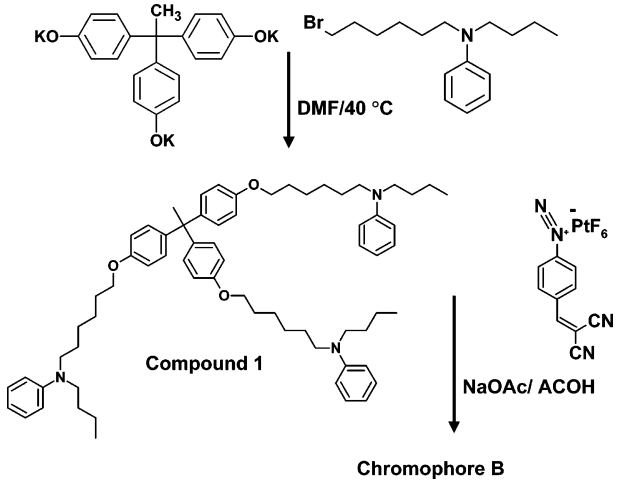

Laboratories, NJ. Thermal analysis was performed under N_2 on a Perkin-Elmer DSC-7 at a heating rate of 10 °C/min. The dipole moment of the chromophore was obtained by measuring the differential capacitance as a function of concentration. Measurements using *p*-dioxane solutions were performed at 1 kHz, using a high-resolution capacitance bridge.

Synthesis of the Branched Chromophores. Chromophore A was synthesized and characterized following the procedure reported in our previous publication (Figure 1).[3] Chromophore B is a new branched azobenzene chromophore with a stronger dicyanovinyl acceptor group. Synthesis of this chromophore is analogous to chromophore B (Scheme 1).

(Dicyanovinyl)benzenediazonium hexafluorophosphate was synthesized following the procedure outlined in ref 8. ^{1}H NMR: CD_3CN: $\delta = 8.30$ (d, 2H), 8.60 (d, 2H).

Compound **1** was synthesized following the previously published procedure. Compound **1** (0.23 g, 0.23 mmol) was dissolved in 5 mL of AcOH at room temperature, and 0.25 g (0.76 mmol) of the (dicyanovinyl)benzenediazonium hexafluorophosphate was added to the above solution. 0.13 g (1.52 mmol) of NaOAc was added in two portions, and the mixture was stirred overnight. The dark blue solution was extracted with dichloromethane and washed with $NaHCO_3$, and the solvent was evaporated under vacuum. The crude solid was purified by silica gel column using 1:1 mixture of dichloromethane:ethyl acetate as solvent to obtain 3.2 g (90%) of chromophore B as purple solid. ^{1}H NMR: $CDCl_3$: $\delta = 0.96$ (m, 9H), 1.25−1.75 (br, 36H), 1.87 (s, 18H), 2.08 (s, 3H), 3.20−3.30 (br, 8H), 3.3−3.5 (br, 8H), 3.94 (m, 6H), 6.59 (d, 6H), 6.64 (d, 4H), 6.75 (d, 6H), 6.98 (d, 6H), 7.08 (d, 3H), 7.16 (t, 6H), 7.64 (d, 3H), 7.73 (d, 4H), 7.86 (t, 6H)].

Table 1. Compositions of Blends Investigated

PVK (wt %)	ECZ (wt %)	chromophore (wt %)	TNF (wt %)	T_g (°C)
47	47	5 (DR 1)	1	65.7
42	42	15 (A)	1	64.6
42	42	15 (B)	1	57.7

Sample Preparation. The poly(vinylcarbazole) (PVK) (secondary standard), ethylcarbazole (ECZ), trinitrofluorenone (TNF), and Disperse Red 1 (DR1) were purchased from Aldrich. Ethylcarbazole is a plasticizer, and TNF is a photosensitizer used for charge generation in PVK. The chromophore, PVK, TNF, and ECZ in specific compositions (Table 1) were dissolved in methylene chloride, filtered with a 0.2 μm syringe filter, and then dripped onto indium tin oxide (ITO)-coated glass electrodes. The glass electrodes were heated to accelerate solvent evaporation and then placed in a vacuum oven. After 4 h the coated electrodes were removed from the oven, covered with a top electrode, and rapidly cooled to form a bubble-free and optically transparent photorefractive polymer film of ~100 μm thickness.

Photorefractive Characterization. Photorefractive characterization consisted of two-beam coupling and diffraction efficiency measurements.[6] Two-beam coupling measurements were used to confirm the presence of the photorefractive effect. Diffraction efficiency experiments were used to probe grating evolution and are discussed in detail below. The two-beam coupling gain coefficient Γ was measured using two p-polarized laser beams intersecting in the polymer film at external angles of 60° and 30° (with respect to the film normal) with a power density of 200 mW/cm^2.

Orientational Response Measurements. The dynamic response of the chromophores to the applied field can be probed by measuring the intensity of a laser beam that passes through the polymer film while placed between crossed polarizers. This transient-ellipsometric technique has been used to examine the reorientation dynamics of several photorefractive polymer systems and is an efficient technique for evaluating the contributions of chromophore orientational dynamics to the overall dynamic response of photorefractive polymer systems.[7]

The laser was a temperature and power stabilized 676 nm (for DR1 and chromophore A blends) or 780 nm (for chromophore B blends) laser diode. The orientation of the linearly polarized output was adjusted with a waveplate, producing a beam polarized at 45° to the plane of incidence. The polymer film was oriented at 45°. The transmitted intensity was measured with a Si amplified photodetector and digital oscilloscope interfaced to a computer-based data acquisition system. A poling step voltage was applied to the film, and the transmitted laser intensity was recorded until no further changes in the signal were detected, indicating steady-state chromophore orientation. The poling voltage was removed,

and the transmitted signal was again recorded as the chromophores relaxed to an isotropic orientational distribution.

Measurement of Photorefractive Grating Evolution. Degenerate four-wave mixing was used for measuring photorefractive diffraction efficiency $\eta(t)$. Two s-polarized laser beams overlap in the polymer blend and write a photorefractive index grating which is probed by a weaker, p-polarized beam counterpropagating to one of the writing beams. The beams were 676 nm for DR1 and chromophore A blends and 780 nm for chromophore B blends. The writing beams were incident at external angles of 60° and 30° with respect to the sample normal with a power density of 200 mW/cm^2; the probe beam had a power density 25 mW/cm^2. At $t = 0$ s, a step voltage was applied to the film and shutters opened applying the write and probe beams. The scattered probe intensity was measured until the photorefractive index grating reached steady state. Diffraction efficiency is defined as $\eta = I_{\text{scattered}}/I_{\text{incident}}$, where I_{incident} is the probe beam intensity measured before entering the film and $I_{\text{scattered}}$ is the probe intensity scattered from the grating.

Results and Discussion

In the photorefractive effect, optical irradiation of the polymer blend by an intensity grating generates photoionized charge, which is spatially redistributed by an externally applied electric field. The vector sum of the space charge field and applied field generates a refractive index grating via the electrooptic chromophore, while periodic alignment of the same dipolar chromophore spatially modulates the birefringence, resulting in an additional contribution to the refractive index grating. Photorefractive index gratings are unique in that the spatial phase shift between the optical intensity grating and the index grating can give rise to asymmetric energy exchange between two laser beams overlapping in a photorefractive polymer. This energy exchange is referred to as two-beam coupling, and it is the signature of photorefractive index gratings.

To explore photorefractive effects using branched azobenzene chromophores, thin films with T_g in the 55−70 °C range were prepared (Table 1). We synthesized two EO chromophores, chromophore A and chromophore B. Chromophore A is a branched analogue of DR1 designed to have increased solubility compared to DR1 in aromatic host such as PVK. Chromophore B has a dicyanovinyl acceptor end, which is likely to further increase the compatibility with PVK host and exhibit a higher r_{33} compared to chromophore A. Electro-optic characterization of chromophore A has been reported earlier,[3] while chromophore B is a new chromophore characterized in this study. Chromophore A was dissolved in 12 wt % solution of APC in cyclopentanone [4.8×10^{20} chromophore molecules/g of polymer], spin-coated on ITO substrate, and dried overnight. Contact poling at 135 °C resulted in an r_{33} value of 6−7 pm/V at 1550 nm. No significant relaxation was observed at room temperature, as the r_{33} value remained constant at 6−7 pm/V over the period of 3 months. Chromophore B samples were prepared and poled identical to chromophore A and exhibited an r_{33} value of 14 pm/V. This is expected as dicyanovinyl is a stronger acceptor group than nitro.[8] In PVK, for example, we observed that blends could be loaded up to 20 wt % with either branched chromophore. The film quality was excellent, with minimal void and/or aggregation problems. The monomeric analogue DR1, however, could be blended only in a 5−7 wt % range and was considerably more difficult to process in bubble-free form. Two-beam coupling experiments clearly showed the presence of photorefractive gratings in both blends, with chromophore B blends showing the most promising photorefractive activity at 780 nm.

Figure 2a shows two-beam coupling in a chromophore A blend at 80 V/μm with $\Gamma = 14.7$ cm^{-1} at a wavelength of 676 nm. In general, two-beam coupling in chromophore A blends was unstable on longer time scales (i.e., >30 s). Two-beam coupling was not observed below ~70 V/μm, while fields greater than 90 V/μm resulted in dielectric breakdown. Figure 2b shows two-beam coupling in a chromophore B blend. Since the absorption peak of the chromophore B blend is at 650 nm, two-beam coupling experiments were performed at 780 nm. Beam coupling was stable over the experimental time scale (~1 h) and was observed over a range of applied fields from a minimum of 33 V/μm to a maximum of 73 V/μm, above which caused dielectric breakdown. The steady-state two-beam coupling gain coefficient as a function of applied field is shown in Figure 2c. The maximum two-beam coupling gain coefficient was 13 cm^{-1} at 73 V/μm. Since the absorption coefficient is 7.6 cm^{-1} at 780 nm, this blend exhibits a 6.4 cm^{-1} net two-beam coupling gain.

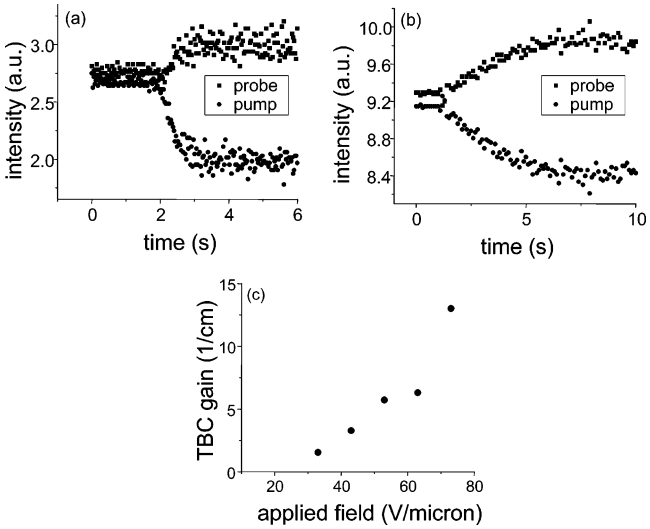

Figure 2. (a) Two-beam coupling in chromophore A blend at 676 nm with 80 V/μm applied field. (b) Two-beam coupling in chromophore B blend at 780 nm with 73 V/μm applied field. (c) Steady-state two beam coupling coefficient of chromophore B blend at 780 nm as a function of applied field.

For comparison, blends containing the monomeric analogue DR1 were also prepared and optically characterized. We observed electric field-induced poling and relaxation in PVK:ECZ:TNF:DR1 blends, while steady-state two-beam coupling was not measurable.

Further insight can be gained by examining the dynamics of photorefractive gratings, which proceed according to several processes: (1) optically induced charge generation, (2) charge transport in external electric field, (3) charge trapping and establishment of space-charge field, (4) refractive index change via electro-optic response to local electrostatic field, and (5) refractive index change due to chromophore reorientation in local electrostatic field. For a given space-charge field, electrooptic index gratings form considerably faster than grating contributions from chromophore reorientation. As a result, the time scales of charge generation and transport relative to that of chromophore reorientation determine the rate-limiting process in the rise time of photorefractive index gratings. An efficient method for identifying such rate-limiting processes is to compare the time-dependent photorefractive diffraction efficiency (i.e., processes 1−5 collectively) with measurements of chromophore reorientation.[9]

(A) Electric-Field-Induced Chromophore Orientation. Electric-field-induced chromophore orientation is a necessary condition for the photorefractive effect in a polymer. At room

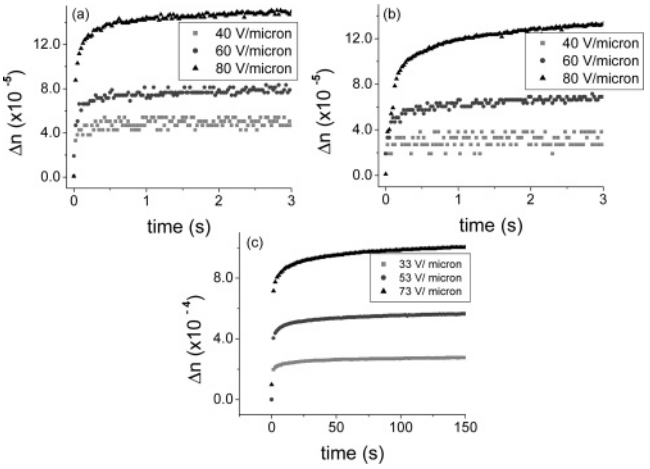

Figure 3. Electric-field-induced birefringence of (a) DR1, (b) chromophore A, and (c) chromophore B blends described in Table 1.

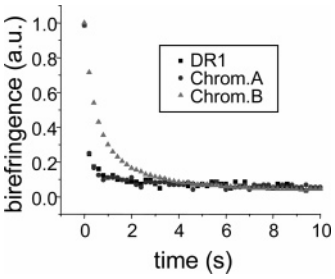

Figure 4. Comparison of relaxation of electric-field-induced birefringence of three blends in Table 1. Blends were poled at 70 V/μm, and poling field was then removed at $t = 0$ s.

temperature, low-T_g polymer blends are optically isotropic since there is no preferred orientation for the dipolar chromophores. Application of an external electric field will remove this isotropy by causing partial alignment of the orientationally mobile chromophores, resulting in an electric-field-induced birefringence. For clarity, a limited number of data points are displayed in the data for induced birefringence of each blend (Figure 3). In all cases, sufficient time was allowed for the chromophore orientation to reach steady state and subsequently relax. Figure 4 compares the relaxation behavior of the three blends following poling and removal of the poling field at $t = 0$ s.

A biexponential of the form $y = y_0 + A_1e^{-t/T_1} + A_2e^{-t/T_2}$ best fit the poling and relaxation data. Although a limited number of data points are displayed (Figure 3), the actual number used for the numerical fits was $\sim 10^5$ data points per curve. This ensures data near $t = 0$ is accurately represented by the fits. Table 2 shows the fitting parameters for the three blends poled and subsequently allowed to relax to the isotropic state. For all three blends, the poling process has a dominant fast component (A1) and a secondary, slower component (A2); this behavior is commonly observed in low-T_g blended photorefractive polymers.[10] Normalized plots of Figure 3 (not shown) indicate that the time constants for a given chromophore are independent of poling field over the range of fields tested.

The orientation of the chromophores during poling is likely governed by the compatibility of the chromophore with the PVK host and the bulk of the chromophore itself. As discussed previously, the branched chromophores A and B offer improved compatibility with aromatic polymer hosts over their monomeric analogues. Both the branched chromophores offered similar compatibility with PVK. As the measured T_g of chromophore B blend is significantly lower (Table 1) than chromophore A,

Table 2. Fit Parameters Comparing DR1, Chromophore A, and Chromophore B Electric-Field-Induced Poling and Relaxation

	A_1	T_1 (s)	A_2	T_2 (s)
Poling Data[a]				
DR1	0.8	0.4	0.2	37.8
chromophore A	0.7	0.5	0.3	19.4
chromophore B	0.7	1.1	0.3	61.5
Decay Data				
DR1	0.86	0.09	0.12	2.58
chromophore A	0.90	0.09	0.08	2.93
chromophore B	0.85	2.30	0.15	35.7

[a] External field was 80 V/μm for DR1 and chromophore A and 73 V/μm for chromophore B.

Table 3. Fit Parameters Comparing Photorefractive Diffraction Efficiency Evolution in DR1, Chromophore A, and Chromophore B Blends with External Fields[a]

PR rise time data	A_1	T_1 (s)	A_2	T_2 (s)
DR1	0.78	2.70	0.22	81.39
chromophore A	0.66	1.99	0.34	47.48
chromophore B	0.82	11.94	0.18	231.0

[a] External field was 80 V/μm for DR1 and chromophore A and 73 V/μm for chromophore B.

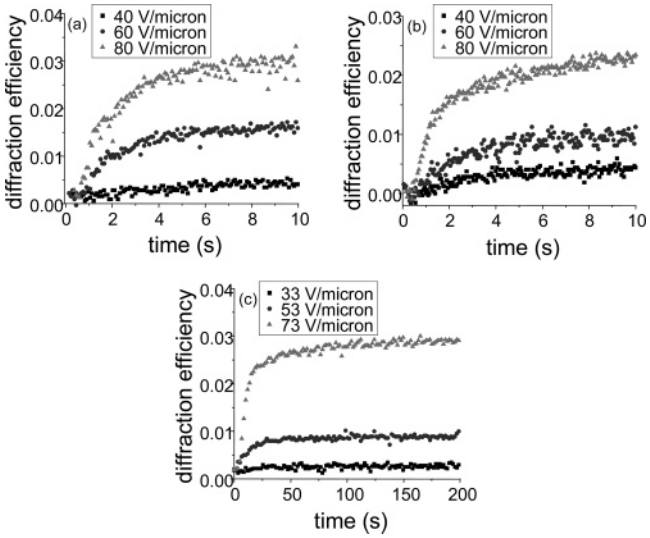

Figure 5. Photorefractive diffraction efficiency of (a) DR1, (b) chromophore A, and (c) chromophore B blends described in Table 1. External field and write beams are applied at $t = 0$ s.

the difference in time constants is most likely a reflection of their respective bulks. As shown in Table 2, the poling time constants T_1 and T_2 for chromophore B are a factor 2−3 times longer than chromophore A; for relaxation, the chromophore B time constants extend to more than a factor of 10 longer than those for chromophore A.

(B) Photorefractive Diffraction Efficiency. Figure 5a−c shows the transient photorefractive diffraction efficiency for the three polymer blends. For clarity, only a limited number of data points are displayed, while the complete data set was used for fitting. The diffraction efficiency for all blends exhibited biexponential behavior. The fit parameters are shown in Table 3 and indicate the characteristic times for photorefractive grating formation are longer than those for chromophore orientation, suggesting that charge generation and transport are the rate-limiting processes. For example, the photorefractive time constants T_1 and T_2 for the chromophore B blend increased by nearly a factor of 11 and 7, respectively, over the time constants measured for purely orientational processes.

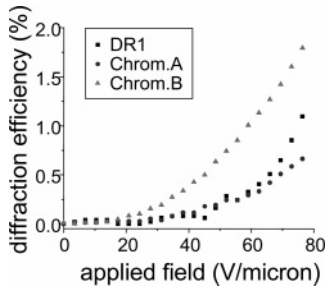

Figure 6. Comparison of the steady-state external diffraction efficiency of three blends in Table 1.

Figure 6 shows the absolute steady-state diffraction efficiency for the three blends as a function of applied field. Although blends containing DR1 exhibited a 0.5% external diffraction efficiency at 80 V/μm, no steady-state two-beam coupling signal was observed. This suggests that grating formation in DR1 blends is dominated by photoisomerization processes, consistent with the results of earlier investigations.[11−14] For chromophore B blends, both the steady-state external diffraction efficiency and two-beam coupling gain increased with applied field, indicating that the chromophore is orientationally mobile in the polymer host and also that spatially modulated birefringence contributes to the overall refractive index modulation.

Summary

In summary, we have demonstrated branched azobenzene chromophores are compatible with aromatic hosts such as PVK, and they exhibit photorefractive index gratings and two-beam coupling in PVK host polymer. Our previous morphological studies of these polar branched chromophores suggest that their enhanced compatibility with aromatic polymer hosts leads to more uniform dispersal, which in turn enables the orientational enhancement (via spatially modulated birefringence) and electrooptic effects essential for the photorefractive effect. When compared with their monomeric analogues, branched chromophores could be blended over a broader range of concentrations and formed into higher quality optical films; these films have retained their optical clarity for one year with no special handling precautions. A new branched chromophore with an EO coefficient of 14 pm/V was synthesized and exhibited photorefractive two-beam coupling over a range of applied fields, including a net two-beam amplification coefficient of 6.4 cm^{-1} at 780 nm.

Acknowledgment. P.G. acknowledges the support of NSF-CAREER 0449688. D.J.M. acknowledges the support of NSF-RUI 0504105.

References and Notes

(1) Zhang, C.; Dalton, L.; Oh, M.; Zhang,; Steier, W. H. *Chem. Mater.* **2001**, *13*, 3043.
(2) Shi, Y.; Zhang, H.; Bechtel, J. H.; Dalton, L. R.; Robinson, B. H.; Steier, W. H. *Science* **2000**, *288*, 119.
(3) Gopalan, P.; Katz, H. E.; McGee, D. J.; Erben, C.; Zielinski, T.; Bousquet, D.; Muller, D.; Grazul, J.; Ollson, Y. *J. Am. Chem. Soc.* **2004**, *126*, 1741.
(4) Ma, H.; Liu, J.; Suresh, S.; Liu, L.; Kang, S.; Haller, M.; Sassa, T.; Dalton, L. R.; Jen, A. K.-Y. *Adv. Funct. Mater.* **2002**, *12*, 565.
(5) Moerner, W. E.; Silence, S. M.; Hache, F.; Bjorklund, G. C. *J. Opt. Soc. Am. B* **1994**, *11*, 320.
(6) Kippelen, B.; Meerholtz, K.; Peyghambariam, N. In *Nonlinear Optics of Organic Molecules and Polymers*; Nalwa, H. S., Miyata, S., Eds.; CRC Press: Boca Raton, FL, 1997; pp 492−505.
(7) Binks, D. J.; Khand, K.; West, D. P. *J. Appl. Phys.* **2001**, *89*, 231.
(8) Sohn, J. E.; Singer, K. D.; Kuzyk, M. G.; Holland, W. R.; Katz, H. E.; Dirk, C. W.; Schilling, M. L.; Comizzoli, R. B. In *Nonlinear Optical Effects in Organic Polymers I*; Messier, J., Ed.; Kluwer Academic Publishers: Dordrecht, 1989; p 291.
(9) Herlocker, J. A.; Ferrio, K. B.; Hendrickx, E.; Guenther, B. D.; Mery, S.; Kippelen, B. *Appl. Phys. Lett.* **1999**, *74*, 2253.
(10) Bittener, R.; Brauchle, C.; Meerholz, K. *Appl. Opt.* **1998**, *37*, 2843.
(11) Nishida, F.; Tomota, Y. *J. Appl. Phys.* **1997**, *81*, 3348.
(12) Sandalphon; Kippele, B.; Peyghambarian, N.; Lyon, S. R.; Padias, A. B.; Hall, H. K. *Opt. Lett.* **1994**, *19*, 68.
(13) Song, O. K.; Wang, C. H.; Pauley, M. A. *Macromolecules* **1997**, *30*, 6913.
(14) Sekkat, Z.; Wood, J.; Knoll, W. *J. Phys. Chem.* **1995**, *99*, 17226.

MA051772O